

# Folding kinetics of the lipoyl acid bearing domain of human mitochondrial branched chain $\alpha$ -ketoacid dehydrogenase complex

Mandar T. Naik, Yu-Chu Chang, Tai-huang Huang\*

*Institute of Biomedical Sciences, Academia Sinica, Taipei 11529, Taiwan*

Received 19 July 2002; revised 6 September 2002; accepted 9 September 2002

First published online 23 September 2002

Edited by Thomas L. James

**Abstract** A reversible two-step (native state  $\leftrightarrow$  denatured state) folding mechanism based on equilibrium and stopped flow experiments is proposed for urea denaturation of the lipoyl-bearing domain (hbLBD) of human mitochondrial branched chain  $\alpha$ -ketoacid dehydrogenase (BCKD) complex. The results from this circular dichroism (CD) and fluorescence study have ruled out populated kinetic or equilibrium intermediates on folding pathway of this  $\beta$ -barrel domain under experimental conditions. Both studies suggested mono-exponential kinetics without any burst phases. Moreover the thermodynamic parameters  $\Delta G_{H_2O}$  and  $m$  obtained from the kinetic analysis are consistent with the equilibrium measurements.

© 2002 Federation of European Biochemical Societies. Published by Elsevier Science B.V. All rights reserved.

**Key words:** Protein folding; Lipoyl-bearing domain; Branched chain  $\alpha$ -ketoacid dehydrogenase; Maple syrup urine disease; Stopped flow kinetics

## 1. Introduction

Recent years have seen much efforts and anticipation toward understanding the folding phenomenon of all  $\beta$ -sheet proteins. Many single domain proteins from this subclass have been identified to fold by an apparent two-step mechanism [1–8]. Interestingly only a few of them like the small  $\beta$ -barrel cold shock proteins (CspA and CspB) have true two-step kinetics and fast folding capabilities [1,2,4]. Most of the medium size proteins like those with  $\beta$ -trefoil topology are found to have transient intermediates and slow folding rates [7–10]. Collectively, these studies have casted doubt on the notion that populated intermediates along the folding pathway are necessary for efficient folding. The folding mechanism of small proteins lacks significant kinetic traps and perhaps is similar to early folding events of their larger counterparts. The observation that folding can occur without a well-defined pathway of populated intermediates has provided support for the new view of protein folding which emphasizes energy landscapes and multiple paths over single pathway [11,12]. Thus model systems with an ideal two-step mechanism are highly sought for better understanding of the folding mechanism.

$\alpha$ -Ketoacid dehydrogenase complexes are multienzyme assemblages generally made up of at least three main enzymes.

These complexes are also known to have remarkable structural and functional similarities [13,14]. Among these complexes, the human mitochondrial branched chain  $\alpha$ -ketoacid dehydrogenase (BCKD) consists of three main catalytic components: a hetero-tetrameric ( $\alpha_2\beta_2$ ) branched chain  $\alpha$ -ketoacid decarboxylase (E1), a homo-24meric dihydrolipoyl transacylase (E2) and a homo-dimeric dihydrolipoamide dehydrogenase (E3). These enzymes act in tandem and are responsible for catalyzing the oxidative decarboxylation of branched chain  $\alpha$ -ketoacids derived from leucine, isoleucine and valine [15]. The branched chain acyl-CoAs formed in this reaction are further channeled into the Krebs cycle or linked to lipid and cholesterol biosynthesis. In patients with inherited maple syrup urine disease (MSUD) the activity of the BCKD complex is deficient. This results in the accumulation of branched chain  $\alpha$ -ketoacids and leads to severe clinical consequences including fatal ketoacidosis, neurological derangement and mental retardation in survivors [16]. The transacylase or E2 component plays an important dual role in proper structural assembly as well as catalytic activity of BCKD. It consists of three independently folded domains viz. the lipoyl-bearing domain (hbLBD), the E1/E3 binding domain and the inner core domain. hbLBD is an 84 amino acid, small  $\beta$ -barrel domain. It hosts the active site lysyl residue responsible for ‘swinging arm’ coupling mechanism [17] and thus plays a central role in substrate channeling in this mitochondrial complex [18–20]. Recently we have determined the nuclear magnetic resonance (NMR) solution structure of hbLBD and found it to be a flattened  $\beta$ -barrel formed by two four-stranded  $\beta$ -sheets (Fig. 1) [20]. It has a sole tryptophan residue, which is advantageous as an intrinsic fluorescence probe to study conformational changes. In the present investigation we report kinetics of urea denaturation using circular dichroism (CD) and fluorescence measurements for this interesting domain.

## 2. Materials and methods

### 2.1. Reagents

Specially prepared reagent grade urea was purchased from Nacalai Tesque Inc., Japan. Stock urea solution was prepared daily, filtered and degassed by sonication before use. The molarity of urea was determined by refractive index measurements [21]. All solutions were prepared in 50 mM potassium phosphate buffer of pH  $7.5 \pm 0.1$  containing 100 mM sodium chloride.

### 2.2. Protein preparation

An expression plasmid (pET28hLBD-His) was transformed in BL21(DE3) strain of *Escherichia coli* under the control of T7 promoter. To facilitate protein expression and purification the recombi-

\*Corresponding author. Fax: (886)-2-2788 7641.

E-mail address: [bmthh@ibms.sinica.edu.tw](mailto:bmthh@ibms.sinica.edu.tw) (T.-h. Huang).

nant domain was constructed to contain a total of 93 amino acids including an extra methionine residue at the N-terminus and a leucine, a glutamic acid along with six histidines at the C-terminus. The protein was first purified by Ni-nitrilotriacetic acid (NTA) affinity chromatography and then by fast protein liquid chromatography (FPLC) using Sephacryl S-100 column. Its purity was found to be more than 95% by gel electrophoresis. The concentration of protein was determined from its molar extinction coefficient of  $\epsilon_{280} = 12090$ .

### 2.3. Equilibrium studies

All titration experiments were carried out with 6  $\mu\text{M}$  hbLBD in 1.0 cm quartz square cuvettes thermostated to  $22.0 \pm 0.1^\circ\text{C}$  at constant pH  $7.5 \pm 0.1$ . Aviv CD spectrometer model 202 with temperature and stir control units in conjugation with auto titrator was used for following ellipticity changes at 228 nm (bandwidth 1 nm and averaging time 1 s). Fluorescence measurements were done manually on Hitachi F-4500 fluorescence spectrophotometer with excitation and emission wavelengths of 295 and 320 nm respectively (slit width 2.5 nm and scan speed 1 nm/s). The equilibrium unfolding data were normalized after baseline correction to give the fraction of unfolded ( $F_u$ ) and analyzed for two-state model by non-linear regression assuming a linear dependency of  $\Delta G_{\text{H}_2\text{O}}$  (unfolding free energy) and  $m$  (degree of hydrophobic exposure upon unfolding) on urea concentration [22].

$$F_u = \frac{e^{\left(\frac{-\Delta G_{\text{H}_2\text{O}} + m[\text{urea}]}{RT}\right)}}{1 + e^{\left(\frac{-\Delta G_{\text{H}_2\text{O}} + m[\text{urea}]}{RT}\right)}} \quad (1)$$

### 2.4. Kinetics studies

Stopped flow kinetics measurements were made on Aviv CD spectrometer model 202 with stopped flow accessory having simultaneous CD and fluorescence data collection capabilities of variable data collection rates. All experiments were performed at  $22.0 \pm 0.1^\circ\text{C}$  and pH  $7.5 \pm 0.1$  by single denaturant concentration jump technique. The kinetics was followed separately for ellipticity changes at 228 nm and fluorescence intensity changes for excitation at 295 nm using cut off filter of 320 nm. The bandwidth of 2 nm was used in both measurements. The dead time of mixture assembly was determined by the test reaction between 8-hydroxyquinoline and magnesium ion [23].

Urea refolding reactions were initiated by a 10-fold dilution of 7.94 M urea denatured hbLBD solution with appropriate urea/buffer solution to give the desired final concentration. Unfolding reactions were conducted similarly by dilution of native hbLBD to desired high-

er urea concentration. The final concentration of protein was 30  $\mu\text{M}$  in all experiments. No amplitude changes were observed in the dead time ( $\sim 2.4$  ms) of the instrument. The resulting folding and unfolding traces were averaged (minimum of five) and analyzed for exponential growth/decay by non-linear least squares algorithm. The logarithm of the observed rates ( $k_{\text{obs}}$ ) was plotted as a function of urea concentration and analyzed for two-step kinetics by non-linear regression [24].

$$\ln k_{\text{obs}} = \ln \left\{ k_{\text{r}(\text{H}_2\text{O})} \cdot e^{(m_{\text{r}}[\text{urea}]/RT)} + k_{\text{u}(\text{H}_2\text{O})} \cdot e^{(m_{\text{u}}[\text{urea}]/RT)} \right\} \quad (2)$$

where  $k_{\text{r}(\text{H}_2\text{O})}$  and  $k_{\text{u}(\text{H}_2\text{O})}$  are the refolding and unfolding rate constants in the absence of urea.  $m_{\text{r}}$  and  $m_{\text{u}}$  represent the dependency of refolding and unfolding rates on urea concentration.

## 3. Results and discussion

The CD spectrum of hbLBD, shown in Fig. 2, insert A, has a prominent positive ellipticity centered at 228 nm with a small shoulder around 205 nm. The presence of a strong positive band at 228 nm may be attributed to the presence of hydrophobic clustering of aromatic amino acids, as shown in Fig. 1 [25]. This band shows negative ellipticity on denaturation. There is an isosbestic point at 202 nm for spectra collected at different urea concentrations. The CD spectrum of the folded hbLBD is unusual in that it lacks a minimum at 218 nm that would be expected for a  $\beta$ -sheet protein [25]. Nevertheless, the composite signal at 228 nm representing secondary and, to a lesser extent, tertiary structural changes can be used to follow global changes in folding environment of hbLBD. The urea-induced unfolding profile for LBD (Fig. 2), as monitored by ellipticity changes at 228 nm, shows that the protein is completely unfolded at urea concentrations greater than 7 M urea. This transition is completely reversible (data not shown). The half-denaturation urea concentration is estimated at  $5.10 \pm 0.03$  M. The  $m$  value, which is a measure of hydrophobic exposure, was found to be  $-1.13 \pm 0.02$  kcal  $\text{mol}^{-1}$   $\text{M}^{-1}$ . The free energy change for unfolding of hbLBD in the absence of urea,  $\Delta G_{\text{H}_2\text{O}}$ , is calculated as  $5.73 \pm 0.12$  kcal  $\text{mol}^{-1}$ .

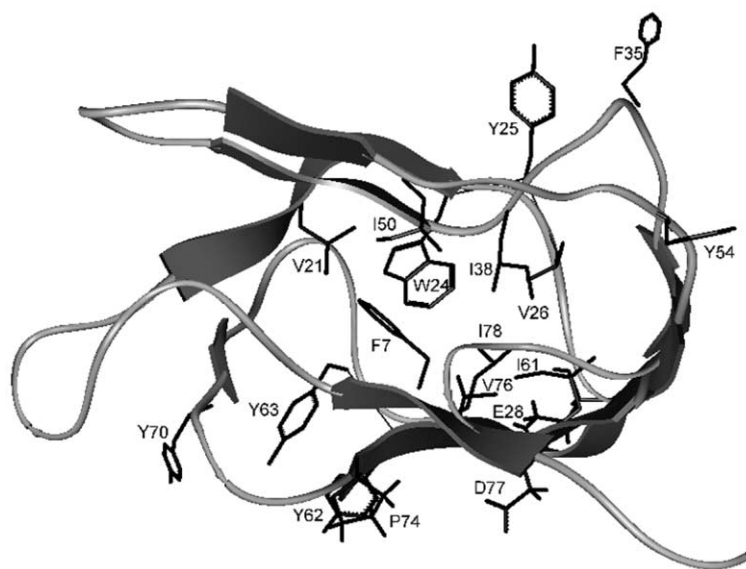


Fig. 1. Ribbon representation of the structure of hbLBD (PDB code: 1k8m), created with InsightII program (Accelrys, San Diego, CA, USA). The domain is a flattened  $\beta$ -barrel comprising of two four-stranded  $\beta$ -sheets. All aromatic residues, residues involved in missense mutation and the hydrophobic residues surrounding Trp<sup>24</sup> are also shown. The amino acids are labeled according to sequence given in the PDB file.

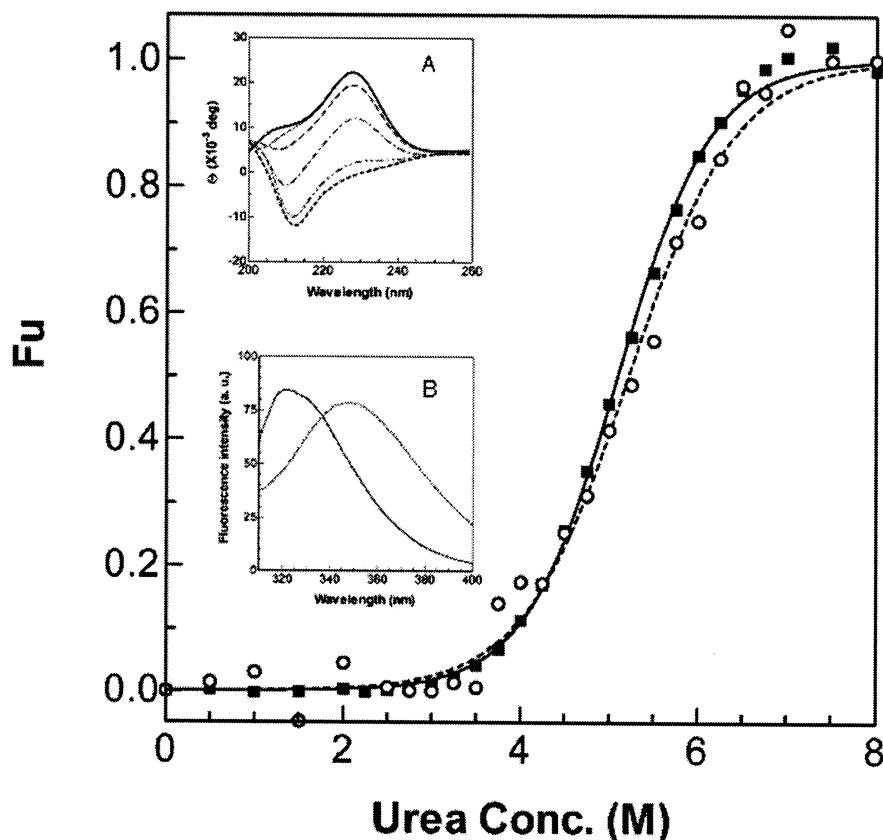


Fig. 2. Urea denaturation of hbLBD at pH 7.5 and 22°C as followed by CD ( $\lambda = 228$ ) (■) and fluorescence ( $\lambda_{\text{ex}} = 295$ ;  $\lambda_{\text{em}} = 320$ ) (○). The fits to Eq. 1 are shown by solid and dotted line respectively. The half-denaturation urea concentrations for hbLBD were found to be 5.10 and 5.22 M by far-UV CD and fluorescence respectively. Inserts: A: CD spectra of hbLBD in the presence of 0 M (solid line), 2 M (dotted line), 4 M (dashed line), 5 M (dash dot line), 6.25 M (dash dot dot line) and 7.5 M (bold dotted line) urea. B: Fluorescence emission spectra of native (solid line) and denatured (dotted line) hbLBD with excitation wavelength of 280 nm. All spectra were recorded at pH 7.5 and 22°C.

The fluorescence of hbLBD on excitation at 280 nm has a typical protein emission hump at 320 nm (Fig. 2, insert B). This band shows a batho-chromic shift to 350 nm on unfolding. This can be mainly attributed to decrease in quenching of the sole tryptophan residue with a minor contribution from five tyrosine residues in hbLBD sequence since little effect on the fluorescence emission was observed when the sample was excited at 295 nm. The large blue shift upon folding reflects the extreme hydrophobicity of the Trp<sup>24</sup> (PDB structure sequence) environment (Fig. 1). The titration curve, as shown in Fig. 2, is almost superimposable with that measured by CD. The half-denaturation urea concentration was  $5.22 \pm 0.08$  M. The  $m$  value and  $\Delta G_{\text{H}_2\text{O}}$  were evaluated as  $-0.98 \pm 0.06$  kcal mol<sup>-1</sup> M<sup>-1</sup> and  $5.14 \pm 0.30$  kcal mol<sup>-1</sup>. They are in good agreement with values obtained by CD. These results strongly suggested that there is no populated equilibrium intermediate(s) in unfolding pathway of hbLBD and the urea-induced

equilibrium denaturation of hbLBD follows a two-step (native state  $\leftrightarrow$  denatured state) mechanism.

We used stopped flow kinetics to detect the presence of transient intermediates. The results of hbLBD unfolding and refolding as monitored by far-ultraviolet (UV) CD and fluorescence are shown in Fig. 3A and B, respectively. The complete signal evolution required nearly 50 s. There are no burst phase ellipticity or fluorescence changes associated with this transition. Traces for both probes can be satisfactorily fitted to single exponential by non-linear regression. The  $F$ -test analysis suggested this to be a mono-exponential process and our observation of residuals of fit supported this conclusion.

The observed rate constant ( $k_{\text{obs}}$ ) for complete unfolding of hbLBD by single urea concentration jump to 7.99 M was found to be  $0.068 \pm 0.001$  s<sup>-1</sup> by both methods. The observed rate constant for similar refolding experiment from 7.94 M urea denatured hbLBD was  $0.25 \pm 0.01$  s<sup>-1</sup>

Table 1  
Summary of equilibrium and kinetic data for hbLBD

Method	$\Delta G_{\text{H}_2\text{O}}$ (kcal mol <sup>-1</sup> )	$m$ (kcal mol <sup>-1</sup> M <sup>-1</sup> )	$k_{\text{r}(\text{H}_2\text{O})}$ (s <sup>-1</sup> )	$m_{\text{r}}$ (kcal mol <sup>-1</sup> M <sup>-1</sup> )	$k_{\text{u}(\text{H}_2\text{O})}$ ( $\times 10^{-3}$ s <sup>-1</sup> )	$m_{\text{u}}$ (kcal mol <sup>-1</sup> M <sup>-1</sup> )
Equilibrium CD	$5.73 (\pm 0.12)$	$-1.13 (\pm 0.02)$	–	–	–	–
Equilibrium fluorescence	$5.14 (\pm 0.30)$	$-0.98 (\pm 0.06)$	–	–	–	–
Kinetic CD <sup>a</sup>	$4.73 (\pm 0.04)$	$-0.89 (\pm 0.03)$	$0.49 (\pm 0.03)$	$-0.44 (\pm 0.02)$	$0.15 (\pm 0.04)$	$0.45 (\pm 0.02)$
Kinetic fluorescence <sup>a</sup>	$4.17 (\pm 0.04)$	$-0.88 (\pm 0.03)$	$0.39 (\pm 0.03)$	$-0.48 (\pm 0.03)$	$0.32 (\pm 0.08)$	$0.39 (\pm 0.02)$

<sup>a</sup> $\Delta G_{\text{H}_2\text{O}} = -RT \ln(k_{\text{u}(\text{H}_2\text{O})}/k_{\text{r}(\text{H}_2\text{O})})$ ;  $m = m_{\text{r}} - m_{\text{u}}$ .

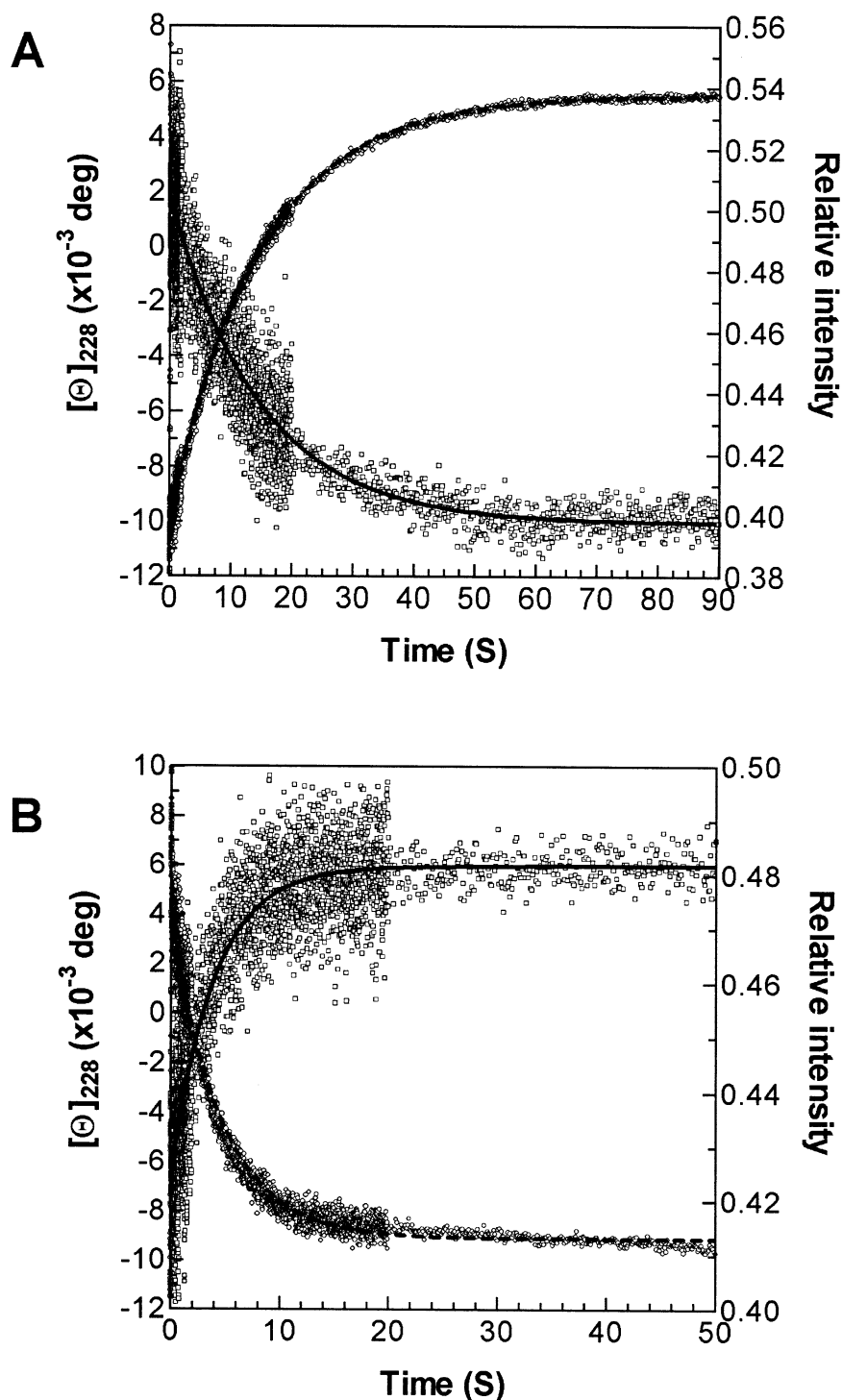


Fig. 3. Unfolding (A) and refolding (B) stopped flow traces for hLBD following a 10-fold dilution. The CD ( $\square$ ) and fluorescence ( $\circ$ ) data were acquired simultaneously in four time domains of varying data collection rates ranging from 1000 points/S ( $t < 20$  s) to 10 points/s ( $t > 20$  s). The mono-exponential fit for CD ( $\lambda = 228$ ) is shown by solid line while that for fluorescence ( $\lambda_{\text{ex}} = 295$ ;  $\lambda_{\text{em}} < 320$ ) by dotted line.

and  $0.21 \pm 0.00 \text{ s}^{-1}$  by far-UV CD and fluorescence respectively. These values though are in perfect agreement within experimental errors. They account for a refolding time constant of 4.3 s (averaged value) for hLBD. This value is in good agreement with the fast phase of previously reported  $\beta$ -trefoil proteins. The equilibrium studies on the folding of this subclass of proteins suggested a two-step mechanism

[5–8], but except a recent report on hisactophilin [5] most of the other members of this subclass have kinetic intermediates on folding pathway [8–10].

In order to establish the rigorous kinetic criteria of a two-step mechanism, we analyzed the logarithm of observed rate constant,  $\ln k_{\text{obs}}$ , as a function of urea concentration using Eq. 2 (Fig. 4). Our results showed a linear relationship be-

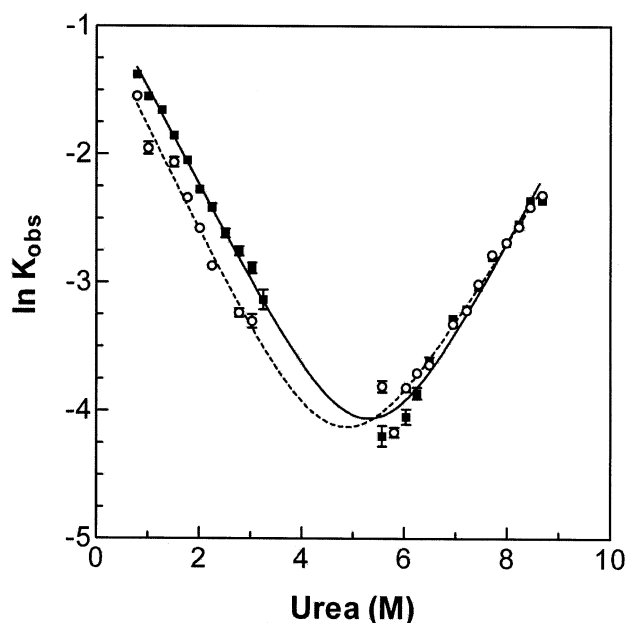


Fig. 4. The chevron plots: Plot of  $\ln k_{\text{obs}}$  against the urea concentration for CD (■) and fluorescence (○) data. The non-linear regression fit to Eq. 2 is shown by solid line for CD while by dotted line for fluorescence. The error bars indicate the statistical error from exponential fitting.

tween logarithm of rate constant and denaturant concentration. The resulting fit resembles a perfect 'V' shape. Moreover the results from far-UV CD are in good agreement with those from fluorescence analysis. This indicates concomitant recovery of both secondary and tertiary structures of hbLBD. All these observations strongly suggested a two-step kinetics without any populated transient intermediates. The kinetic parameters are summarized in Table 1. The apparent equilibrium stability,  $\Delta G_{\text{H}_2\text{O}}$ , estimated from the ratio of refolding and unfolding rate constants agrees within experimental error with the equilibrium analysis. The  $m$  value from both probes is also in good agreement with the value deduced from equilibrium analysis. This is an additional and strong proof for two-step kinetics of hbLBD.

hbLBD from BCKD, as well as from pyruvate dehydrogenase complex (PDC), are M2 auto antigens in patients with primary biliary cirrhosis. Nearly 63 mutations, a majority of which affect E1 $\alpha$  or E2 loci, are identified in BCKD complex gene of MSUD patients [14]. There are six missense mutations (E28del, I38M, P74R, P74L, D77Y, and I78t) detected in the hbLBD that affect stability of the E2 subunit and are without effect on lipoic acid incorporation in hbLBD [16]. The hbLBD structure shows that the two residues Ile<sup>38</sup> and Ile<sup>78</sup> are buried inside the hydrophobic core and are likely to contribute significantly to the stability of the domain. Therefore, the pathological consequence of these two mutations could potentially be due to the effect on stability and folding of the molecule. The other three mutated residues are surface residues on sheet S2. Pro<sup>74</sup> is the first residue in strand 8. Due to the unique backbone structure in proline, a mutation in this residue can have significant effect on the overall folding. Glu<sup>28</sup> is located in the loop between strands  $\beta_2$  and  $\beta_3$ . An in-frame deletion in the residue results in the absence of E2 protein (data not shown), suggesting this residue also has profound effects on folding of the E2 chain. Asp<sup>77</sup> resides in the middle of strand 8, and its side chain is also on the surface. Whether the pathological effect of this residue is due to its involvement

in recognition with other components of the BCKD complex or due to perturbation on the protein folding remains to be elucidated. The current work is instrumental in planning future study to estimate consequences of these mutations on folding and stability of hbLBD and its effect on overall function of BCKD.

*Acknowledgements:* We thank Jacinta L. Chuang and Dr. David T. Chuang for providing the hbLBD clone and for stimulating discussions. This project is supported by a grant from the National Science Council of the Republic of China (NSC90-2113-M-001-023).

## References

- [1] Schindler, T. and Schmid, F. (1996) *Biochemistry* 35, 16833–16842.
- [2] Schindler, T., Herrler, M., Marahiel, M. and Schmid, F. (1995) *Nat. Struct. Biol.* 2, 663–673.
- [3] Perl, D., Welker, C., Schindler, T., Schroder, K., Marahiel, M., Jaenicke, R. and Schmid, F. (1998) *Nat. Struct. Biol.* 5, 229–235.
- [4] Reid, K., Rodriguez, H., Hillier, B. and Gregoret, L. (1998) *Protein Sci.* 7, 470–479.
- [5] Viguera, A.R., Martinez, J.C., Filimonov, V.V., Mateo, P.L. and Serrano, L. (1994) *Biochemistry* 33, 2142–2150.
- [6] Liu, C., Gaspar, J.A., Wong, H.J. and Meiering, E.M. (2002) *Protein Sci.* 11, 669–679.
- [7] Burns, L.L., Dalessio, P.M. and Ropson, I.L. (1998) *Proteins Struct. Funct. Genet.* 33, 107–118.
- [8] Samuel, D., Kumar, T.K.S., Balamurugan, K., Lin, W.-Y., Chin, D.-H. and Yu, C. (2001) *J. Biol. Chem.* 276, 4134–4141.
- [9] Varley, P., Gronenborn, A., Christensen, H., Wingfield, P.T., Pain, R.H. and Clore, G.M. (1993) *Science* 260, 1110–1113.
- [10] Estape, D. and Rinas, U. (1999) *J. Biol. Chem.* 274, 34083–34088.
- [11] Wolynes, P.G., Onuchic, J.N. and Thirumalai, D. (1995) *Science* 267, 1619–1620.
- [12] Dill, K.A. and Chan, H.S. (1997) *Nat. Struct. Biol.* 4, 10–19.
- [13] Reed, L.J. (2001) *J. Biol. Chem.* 276, 38329–38336.
- [14] Yeaman, S.J. (1989) *Biochem. J.* 257, 625–632.
- [15] Chuang, D.T., Chuang, J.L., Wynn, R.M. and Song, J.L. (2001) in: *Encyclopedia of Molecular Medicine Vol. 1* (Creighton, T.E., Ed.), pp. 393–396, Wiley, New York.

- [16] Chuang, D.T. and Shih, V.E. (2001) in: *The Metabolic and Molecular Basis of Inherited Disease* (Scriver, C.R., Beaudet, A.L., Sly, W.S., Valle, D., Vogelstein, B. and Childs, B., Eds.), pp. 1971–2006, McGraw-Hill, New York.
- [17] Perham, R.N. (2000) *Annu. Rev. Biochem.* 69, 961–1004.
- [18] Berg, A. and de Kok, A. (1997) *J. Biol. Chem.* 378, 617–634.
- [19] Radke, G., Ono, K., Ravindran, S. and Roche, T. (1993) *Biochem. Biophys. Res. Commun.* 190, 982–991.
- [20] Chang, C.-F., Chou, H.-T., Chuang, J.L., Chuang, D.T. and Huang, T.-h. (2002) *J. Biol. Chem.* 277, 15865–15873.
- [21] Pace, C.N. (1986) *Methods Enzymol.* 131, 266–280.
- [22] Agashe, V.R. and Udgaonkar, J.B. (1995) *Biochemistry* 34, 3286–3289.
- [23] Brisette, P., Ballou, D.P. and Massey, V. (1989) *Anal. Biochem.* 181, 234–238.
- [24] Jackson, S.E. and Fersht, A.R. (1991) *Biochemistry* 30, 10428–10435.
- [25] Thompson, T.M., Mark, B.L., Gray, C.W., Terwilliger, T.C., Sreerama, N., Woody, R.W. and Gray, D.M. (1998) *Biochemistry* 37, 7463–7477.